

## New Results Using Membrane-Supported Circuits: A Ka-Band Power Amplifier and Survivability Testing

T. M. Weller, L. P. B. Katehi, M. I. Herman,  
P. D. Wamhof, K. Lee, E. A. Kolawa, and B. H. Tai

**Abstract**—This paper describes recent results which pertain to the integration and reliability testing of micromachined, membrane-supported transmission line circuits. These circuits employ a 1.4- $\mu\text{m}$ -thick dielectric membrane to support thin-film conducting lines above an air substrate. With regard to integration, the development of a Ka-band solid state power amplifier (SSPA) is presented. The design includes a membrane-supported Wilkinson power divider/combiner with 0.2 dB loss, along with a commercially available monolithic microwave/millimeter wave integrated circuit (MMIC) amplifier stage. Also reported are tests which investigated the survivability of membrane lines under space qualification conditions. No failures occurred as a result of thermal cycling and vibration testing at levels which reached 39.6 grms.

### I. INTRODUCTION

Transmission lines that are supported by micron-thin dielectric membranes are now being used in the development of advanced microwave circuits. In these designs the substrate is removed using micromachining techniques, resulting in a medium that propagates nearly pure transverse electric magnetic (TEM) modes. Examples of recent work operate from dc to submillimeter-wave frequencies, and include components such as very high- $Q$  inductors, W-band filters, and a 250-GHz band-pass filter [1]–[3]. A variety of topologies has also been investigated, including microstrip, strip-line, and open and shielded coplanar waveguide.

In each demonstration of the membrane-supported circuits, the advantages of the homogeneous air dielectric have been apparent. The absence of dielectric loss and any noticeable dispersion has resulted in performance which exceeds that typically achieved using conventional planar technologies. As a result, membrane-supported circuits show strong potential for applications such as near-earth and deep space communications systems, as well as scientific instrumentation.

In this paper we report on two aspects of membrane-supported lines which, along with the electrical characteristics, are critical to the future system insertion of membrane technology. These aspects are the integration of membrane lines into active device modules, and the survivability of membranes. The former issue was addressed in the development of a Ka-band solid state power amplifier (SSPA). The first phase of the project involved the design of a membrane-supported Wilkinson power splitter and combiner, and the second phase dealt with the addition of an MMIC amplifier stage to the circuit. Important insight pertaining to the implementation of these

Manuscript received December 12, 1995; revised May 24, 1996. This work was supported in part by the University of Michigan and the Jet Propulsion Laboratory, California Institute of Technology, under a contract with the National Aeronautics and Space Administration, through sponsorship of NASA's Office of Advanced Concepts and Technology and Office of Science as well as the Pluto Express Advanced Technology Insertion effort.

T. M. Weller is with the Microwave and Wireless Laboratory, University of South Florida, Tampa, FL 33620 USA.

L. P. B. Katehi is with The Radiation Laboratory, University of Michigan, Ann Arbor, MI 48109 USA.

M. I. Herman, K. Lee, and E. A. Kolawa are with the Jet Propulsion Laboratory, California Institute of Technology, Pasadena, CA 91109 USA.

P. D. Wamhof is with the Core Dynamic Corp., Irvine, CA 91109 USA.

B. H. Tai is with the Department of Chemical Engineering and Materials Science, University of California, Davis, CA 95616 USA.

Publisher Item Identifier S 0018-9480(96)06393-4.

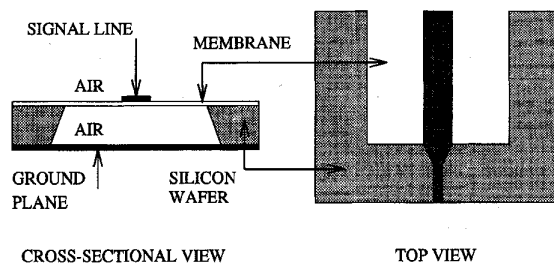


Fig. 1. Illustration of the membrane-supported microstrip line. The top view is a transition from a silicon substrate to the membrane line.

new architectures was gained from this initial effort. A related project centered on thermal and vibration cycling of membrane-supported structures under space-qualification conditions.

### II. WILKINSON POWER DIVIDER/COMBINER

As originally described in [4], the Wilkinson power divider/combiner was implemented using microstrip lines printed on a thin (1.4  $\mu\text{m}$ ) dielectric membrane. The membrane is a tri-layer of  $\text{SiO}_2/\text{Si}_3\text{N}_4/\text{SiO}_2$  which is grown on a silicon wafer using thermal oxidation and low pressure chemical vapor deposition (LPCVD). It is left free-standing by selective chemical etching of the silicon, in a process used to open windows in the substrate beneath the conducting lines.

One of the important design issues associated with the Wilkinson splitter was obtaining a low loss transition between the 50  $\Omega$  silicon input/output lines and the membrane line (Fig. 1). A transition based on impedance matching is impractical since a 50  $\Omega$  membrane line would occupy too much circuit area; assuming a substrate height of 350  $\mu\text{m}$ , a 50  $\Omega$  membrane line is nearly 2 mm wide, compared to a 0.32 mm for a line on silicon. An alternative approach is to utilize a quarter-wavelength transformer to increase the impedance level of the membrane circuits. In this case, the design of the transition must take into account the angled profile of the silicon sidewall which results from the anisotropy of the silicon etchant [5]. The final configuration used a  $\lambda/4$  section of 73  $\Omega$  membrane line, which is 1 mm wide, to transform up to a 106  $\Omega$  reference impedance. The measured insertion loss of this transition was approximately 0.04 dB at 33 GHz.

In order to accommodate integration into the SSPA test fixture, the power divider and the impedance transformers were fabricated on a membrane chip with a surrounding silicon collar (Fig. 2). The layout utilized an 8  $\times$  8 mm<sup>2</sup> membrane, which proved to be quite robust as only 2% (1 out of 50) failed during processing. The fabrication began with the deposition of 212  $\Omega$  thin-film resistors which were 324  $\mu\text{m}$  long and 30  $\mu\text{m}$  wide, using 400- $\text{\AA}$ -thick titanium (20  $\Omega/\text{sq}$ ). The front-side metallization and the removal of the back-side masking (membrane) layer were then completed using standard photolithography techniques. Before the wet-etching, a dicing saw was used to separate the substrate into single rows of 4 circuits, cutting perpendicularly to the input and output 50  $\Omega$  silicon lines. Micromachining was then performed to obtain the free-standing membranes, and scribe lines were simultaneously etched such that the circuits were connected at their corners by 100- $\mu\text{m}$ -wide Si struts. This dicing/scribe line procedure provided a clean profile at the input and output lines, and at the same time minimized the number of pieces handled during etching. To complete the processing, the dividers were separated and mounted to the test fixture using a nonconductive

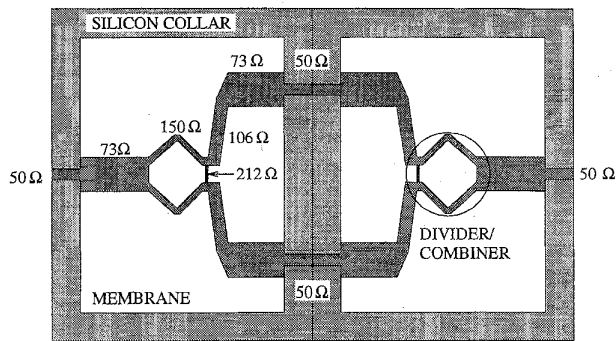


Fig. 2. Layout of the membrane-supported Wilkinson power divider/combiner, shown in a back-to-back configuration.

epoxy. Finally, an aluminum plate was positioned above the circuits to protect the membranes during the SSPA assembly and measurement phase.

The measured results for a back-to-back Wilkinson configuration are given in Fig. 3. This data demonstrates a return loss greater than 22 dB and an insertion loss of 1.2 dB at 33 GHz. Included in Fig. 3 is the isolation between the two output ports, which was determined from an individual circuit by terminating the input port with a 50  $\Omega$  thin-film resistor. Also, since the protective aluminum plate adds capacitive loading to the circuit, its height was chosen as a compromise between minimizing the insertion loss and maximizing the return loss. The optimum height was determined to be 2.7 mm above the circuit.

A detailed breakdown of the performance is given in Table I, showing that the extracted insertion loss for a single divider with 50  $\Omega$  input/output impedance is 0.3 dB. After accounting for the quarter-wave transformers, the power divider itself contributes approximately 0.2 dB. Typical performance for Wilkinson designs at this frequency range, using conventional microstrip, is 0.5–0.9 dB [6].

### III. SOLID STATE POWER AMPLIFIER

The SSPA module consisted of an amplifier power section with a membrane-based Wilkinson divider/combiner on the input and output ports (Fig. 4). On either end of the module were 50  $\Omega$  microstrip lines on alumina, which were used to interface with a Wiltron 3680 K test fixture. The three sections (divider, power stage, combiner) were assembled using a gold plated, split-block test fixture with aluminum for the end pieces and Kovar for the center piece. The Kovar section was used in order to obtain a good match to the thermal expansion of the alumina substrates. In hindsight, adhering the Wilkinson dividers directly to the aluminum blocks was not the optimum method, since thermal expansion mismatches caused some torsion of the silicon collar that surrounds the membrane. Future designs could be improved by first attaching the divider to a larger, Au-plated silicon piece, and/or by using a block material which has a better thermal match to silicon (e.g., Wolfmet TC [7]). After assembly, wire bonds were used to electrically connect the signal lines on the three pieces, and also to contact the output alumina pads.

The Ka-band amplifier section was a simple combination of two commercially available 0.5 W Alpha MESFET-based MMIC chips (SN AA035P2-00). Since large signal data was not available to pick two matched chips, 50  $\Omega$  alumina lines were placed at the input and output of the devices (0.51 cm long) to allow for tuning (Fig. 4). The bias lines for both chips were tied together as in an actual application; therefore, only one gate- and one drain-power supply were required.

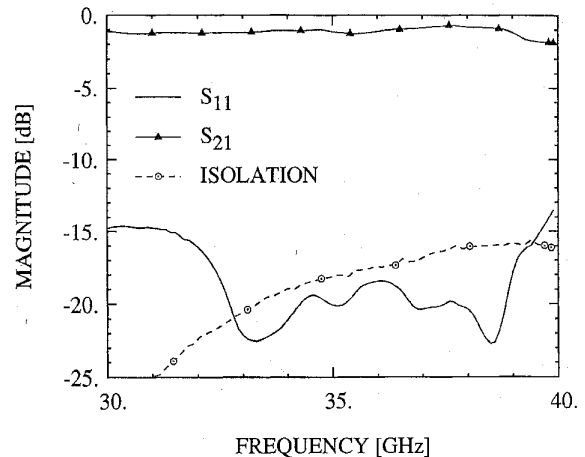


Fig. 3. Measured scattering parameters for the back-to-back Wilkinson power divider shown in Fig. 2. The isolation was measured between the output ports of a single circuit.

Performance data on the SSPA module was taken at several frequencies between 30–35 GHz, and it was found that no tuning was required on either the input or output. For a constant input power drive the circuit gain varied from 4 to 6.5 dB, with a constant output power of around 800 mW (Fig. 5). As shown in Fig. 6, the amplifier exhibited 5.2 dB gain with an output power of 0.85 W and 17% power added efficiency at 33 GHz. This data includes the removal of the alumina lines whose loss is approximately 0.35 dB/cm, but not the extra wirebond interconnects. If we employed a traditional alumina power divider, the output power would have been reduced by approximately 80 to 140 mW, or a factor of up to 16%.

### IV. SURVIVABILITY TESTING

In a project related to the SSPA development, membrane-supported circuit geometries were subjected to space-qualification level survivability testing. The tests were performed at the Jet Propulsion Laboratory, by researchers in the Advanced Materials and Fluid Processes Technology Group. Additional tests on membrane stress characteristics were conducted by the Vibrational Stress Metrology group at JPL [8]. For both sets of preliminary tests, samples with two different membrane sizes (1.8  $\times$  4.8 mm<sup>2</sup> and 2.8  $\times$  7.8 mm<sup>2</sup>) were used.

The tests consisted of alternate series thermal cycling and vibration testing. During each thermal test phase the membrane structures were cycled from  $-65^{\circ}\text{C}$  to  $+150^{\circ}\text{C}$  and inspected optically after 100 and 200 cycles. The specifications for the random vibration tests are given in Table II; the levels given in the table resulted in an overall force of 39.6 grms, and the duration was 180 sec/axis. Finally, in conducting the tests, four separate sequences were employed using four sample circuits in each: vibration/inspect, vibration/thermal/inspect, thermal/vibration/inspect, and thermal/vibration/thermal/inspect.

The results of the thermal and vibration tests were very encouraging as all properly prepared samples survived. Two circuits failed during thermal testing when the micromachined cavities were not adequately vented, and one circuit was damaged due to a documented test operator error. These findings strongly suggest that membrane-supported circuits are capable of surviving a space-flight environment, since the test levels are representative of worst-case launch conditions, i.e., a Titan launch vehicle. A cautionary note is warranted however, since conclusive results will require that a much larger number of samples be tested.

TABLE I  
LOSS BUDGET FOR THE WILKINSON POWER DIVIDER SHOWN IN FIG. 2.  
THE ENTRIES AT THE TOP OF THE TABLE ARE EXPERIMENTALLY DETERMINED VALUES AT 30 GHz

Parameter	Units	Loss	Total
Wire-bond	dB	0.04	
50 Ω microstrip on 10 mil alumina	dB/mm	0.035-0.04	
50 Ω microstrip on 14 mil silicon	dB/mm	0.085	
106 Ω microstrip on membrane (14 mil)	dB/mm	0.025	
Insertion loss of back-to-back divider	dB		1.18
3 Wire-bonds	dB	-0.12	1.06
Loss per divider (divide by 2)	dB		0.53
Addtl. 50 Ω & 106 Ω line	dB	-0.23	0.30
<b>Corrected loss per divider</b>	dB		<b>0.30</b>
Input & Output λ/4 transformers	dB	-0.08	0.22
<b>Loss per divider w/o transitions</b>	dB		<b>0.22</b>

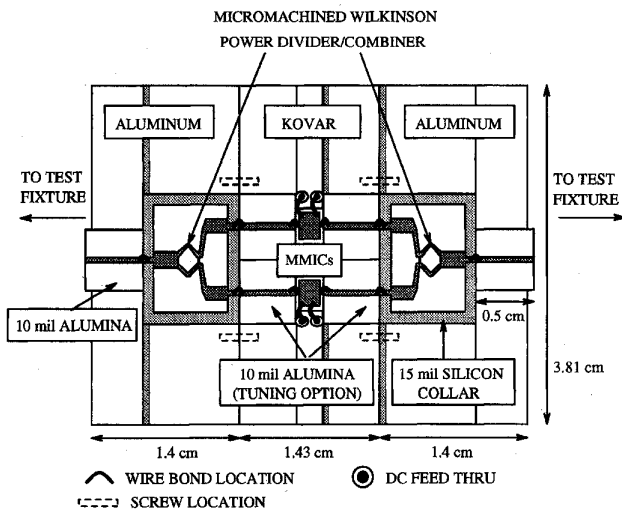


Fig. 4. Ka-band 0.85-W MMIC power amplifier.

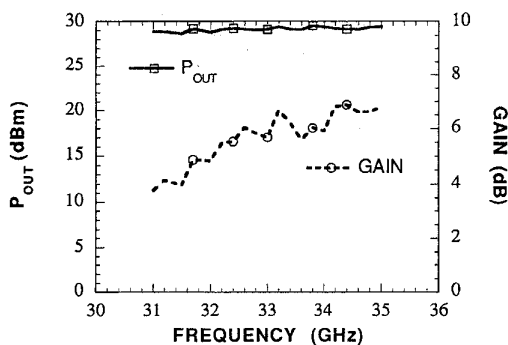


Fig. 5. Frequency response of the Ka-band amplifier with constant input power.

V. CONCLUSION

The RF performance of a membrane-supported microstrip circuit has proven to be excellent compared to that of circuits which are fabricated using traditional planar lines. In this work a Wilkinson power divider was demonstrated which has 0.2 dB insertion loss at Ka-band, compared to typical values ranging from 0.5 to 0.9 dB. Due to the homogeneous air medium, the membrane lines have no

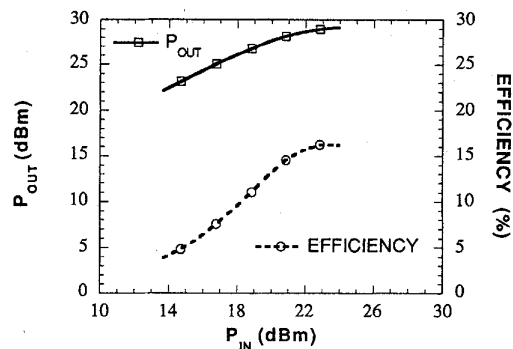


Fig. 6. Gain and power added efficiency of Ka-band amplifier as a function of input drive level.

TABLE II  
RANDOM VIBRATION LEVELS USED IN MEMBRANE TESTING

Frequency (Hz)	Level
20	0.129 g <sup>2</sup> /Hz
20-50	+6 dB/octave
50-2000	0.8 g <sup>2</sup> /Hz

dielectric loss and an extremely wide single-mode bandwidth. For example, a membrane line which is 500 μm wide on a 350 μm substrate sustains a pure TEM mode from dc to at least 320 GHz [9], whereas a similar line on silicon will propagate a higher order mode at 62 GHz. Based on the survivability testing that was described, it also appears that the membrane geometries can withstand the rigors of a launch environment.

The performance advantage of membrane-supported circuits is easily lost, however, if circuit functions are not efficiently implemented. As an example, the compatibility of line geometries going from essentially air to a substrate whose relative permittivity ranges from 2 to 13 becomes a challenge. In this initial work on the Wilkinson divider, it was necessary to step up the impedances and therefore contend with increased circuit dimensions and additional line losses. The obvious solution is to plan the circuit architecture in such a way as to maximize the advantage of the low loss media. In particular to communication systems, this line of thought leads to the implementation of traditional circuit functions such as preselect filters, low noise amplifiers, phase shifters and couplers on a single membrane chip.

## ACKNOWLEDGMENT

The authors would like to express their appreciation for the support by R. Staehle, S. Weinstein, and H. Price of the Pluto Express Pre-Project Office and S. Robertson from the University of Michigan.

## REFERENCES

- [1] C. Y. Chi and G. M. Rebeiz, "Planar microwave millimeter-wave lumped elements and coupled-line filters using micromachining techniques," *IEEE Trans. Microwave Theory Tech.*, vol. 43, no. 4, pp. 730-738, Apr. 1995.
- [2] S. V. Robertson, L. P. Katehi, and G. M. Rebeiz, "W-band microshield low-pass filters," *IEEE Trans. Microwave Theory Tech.*, vol. 2, pp. 625-628, 1994.
- [3] T. M. Weller, L. P. Katehi, and G. M. Rebeiz, "A 250 GHz microshield bandpass filter," *IEEE Microwave Guided Wave Lett.*, vol. 5, no. 5, pp. 153-155, May 1995.
- [4] T. M. Weller, L. P. Katehi, M. I. Herman, and P. D. Wamhof, "Membrane technology (MIST-T) applied to microstrip: A 33 GHz Wilkinson power divider," *IEEE Trans. Microwave Theory Tech.*, vol. 2, pp. 911-914, 1994.
- [5] T. M. Weller, "Micromachined high frequency transmission lines on thin dielectric membranes," Ph.D. Dissertation, Radiation Lab., Univ. of Mich., 1995.
- [6] M. Hamadallah, "Microstrip power dividers at mm-wave frequencies," *Microwave J.*, pp. 116-127, July 1988.
- [7] M & I Materials Ltd., P.O. Box 136, Manchester M60 1AN, England.
- [8] A. Biswas, T. Weller, and L. P. B. Katehi, "Stress determination of micromembranes using laser vibrometry," *Review Sci. Instrum.*, in press.
- [9] K. Sabetfakhri, Univ. of Mich., personal communication.
- [10] B. C. Wadell, *Transmission Line Design Handbook*. Boston: Artech House, 1991, pp. 95-97.

### Axisymmetric Modes of Cylindrical Resonators with Cascaded Inhomogeneous Dielectrics

Jean-Fu Kiang

**Abstract**— A generic numerical scheme is developed to calculate the resonant frequency of axisymmetric modes in an inhomogeneous cylindrical dielectric resonator. The resonator consists of sections of cylindrically stratified dielectrics within a cylindrical waveguide. In each section, the  $TM_{0m}$  and  $TE_{0m}$  waveguide modes are solved by expanding the  $H_\phi$  and  $E_\phi$  components in terms of the eigenmodes in an empty waveguide. The fields in each section are then expanded in terms of these  $TM_{0m}$  and  $TE_{0m}$  modes. The transverse resonance technique is then applied to obtain the resonant frequencies. Comparison with literatures validates the effectiveness of this approach. Results with continuous dielectric profiles are also obtained.

#### I. INTRODUCTION

Cylindrical cavities have been used to cure materials [1], to measure complex permittivity of materials [2], and as a resonator in microwave circuits [3]-[11]. In all these applications, the circular waveguide section forming the cavity contains inhomogeneous dielectrics. For the resonator application, the resonant frequencies of

Manuscript received December 18, 1995; revised May 24, 1996. This work was supported by the National Science Council, Taiwan, ROC under Contract NSC 85-2213-E005-010.

The author is with the Department of Electrical Engineering National Chung-Hsing University, Taichung, Taiwan, ROC.

Publisher Item Identifier S 0018-9480(96)06394-6.

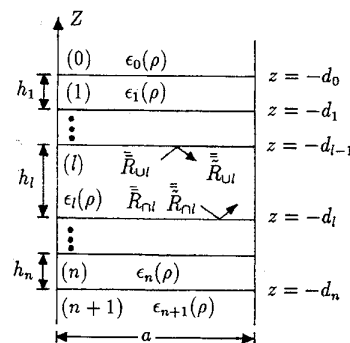


Fig. 1. Geometrical configuration of cascaded circular waveguide sections loaded with inhomogeneous dielectrics.

the dielectric loaded cavity need to be determined precisely. Several coupled dielectric rod or ring resonators can be arranged coaxially in a circular waveguide to form a bandpass filter. The resonant frequencies of the axisymmetric  $TE_{01\delta}$  and  $TM_{01\delta}$  modes have been calculated by using a mode-matching technique [3], [4]. For both modes, the resonant frequencies are below the cutoff frequency of the  $TE_{01}$  waveguide mode. In [5] and [6], the resonant frequency of nonaxisymmetric hybrid modes are calculated by using a similar technique.

In [7], a finite integration technique (FIT) based on the integral forms of Maxwell's equations is proposed to calculate the resonant frequencies of a cavity filled with an inhomogeneous dielectric. A brief summary of mode nomenclature is also provided in [7]. In [8], a variational expression is used to calculate the resonant frequencies of axisymmetric modes where the radial variation of field components are expanded by the first-order finite element (FE) basis functions and the axial variation is expanded in terms of sinusoids. Finite-difference method in the frequency domain [9], finite-difference time-domain (FDTD) method [10], and finite element method (FEM) [11] have also been used.

Mode-matching method proves to be efficient for many canonical resonator structures. For example, the cylindrical dielectric rod and ring in a cylindrical cavity. Usually, the eigenmodes in a stratified medium need to be solved first to represent the field distribution in the later stage. If the dielectric ring consists of many layers or if a dielectric rod has a continuous permittivity profile, conventional mode-matching method becomes tedious or impossible. For such structures, finite element method, FDTD method, and FIT method can be used at the expense of finer grids to express the fields accurately.

In this paper, we will present a generic numeric scheme to solve such problems. First, the eigenmodes in each uniform dielectric loaded waveguide section are obtained by solving a symmetric eigenvalue problem, where dielectrics with continuous profile can also be handled. Reflection matrices at the junctions of waveguide sections are defined to reduce the number of unknowns. Then the transverse resonance technique is applied to obtain the resonant frequencies of the resonators.

#### II. FORMULATION

Fig. 1 shows the configuration of a cylindrical resonator with radius  $a$ , which consists of several sections of circular waveguides loaded with inhomogeneous dielectrics. The permittivity in each layer is a piecewise continuous functions of  $\rho$  and is independent of  $\phi$  and  $z$ .